

The Characterisation of Solids by Adsorption and Immersion Techniques and by AFM/STM

F. Stoeckli,^{a*} D. Hugi-Cleary^a and T. A. Centeno^b

^aChemistry Department, University of Neuchâtel, Av. Bellevaux 51, CH-2000 Neuchâtel, Switzerland

^bInstituto Nacional del Carbon, La Corredoria, E-33080 Oviedo, Spain

Abstract

The surface of porous and non-porous solids can be characterised by a variety of techniques. Basic information is provided by the interpretation of adsorption isotherms, which can be combined with immersion calorimetry. Adsorption in micropores is described by Dubinin's theory, which applies to carbons, as well as other solids, but it appears that this theory can also be extended to non-porous solids. In this case, it takes the form of the Dubinin–Radushkevich and Kaganer (DRK) equation. For a number of systems, a good agreement is found with the BET method and the data obtained from vapour adsorption and from immersion calorimetry shows self-consistency. The structural data derived from adsorption and immersion techniques is also compared with the direct observation of the surface by atomic force and scanning tunnelling microscopies. The relation with the fractal character D of a surface is also considered. © 1998 Elsevier Science Limited. All rights reserved

1 Introduction

The characterisation of solid surfaces can be carried out by a variety of techniques, which depend on the type of information to be obtained. In most cases, the basic information deals with the presence or the absence of porosity, the surface area and the surface energy, which can be derived from the study of the gas–solid and the gas–liquid interfaces. In this respect, the works of Gregg and Sing¹ and of Parfitt and Sing² remain classical references. As shown below, this approach can be combined with

other independent techniques such as high-resolution electron microscopy and, more recently, with atomic force microscopy (AFM) and scanning tunnelling microscopy (STM). This approach provides a coherent description of porous and non-porous solids in general.

Basic information is provided by the physical adsorption of vapours and gases, for which there exists a number of models, ranging from the classical Langmuir and BET equations,¹ essentially valid for non-porous surfaces, to refined approaches described in recent years.³ In the case of microporous solids, the theory of Dubinin,^{4–6} presented exactly 50 years ago, remains one of the most attractive models in view of its simplicity. From a practical point of view, this theory is of great help in filtration technology based on active carbons, where the removal of single components and of binary vapour mixtures from a stream of air can now be predicted with a good accuracy.^{7–9}

Originally developed for active carbons, Dubinin's theory has been extended to zeolites and to other microporous solids. At a later stage, immersion calorimetry has also been included, which provides complementary information for the study of microporous solids.^{5,6,10} As shown by Kaganer¹¹ in the mid-1950s and confirmed by different authors,³ it appears that at low relative pressures ($p/p_s < 10^{-2} - 10^{-3}$), certain systems can also be described by a modification of the Dubinin theory, the so-called equation of Dubinin–Radushkevich and Kaganer (DRK). One finds that the monolayer capacity derived from this approach is often in good agreement with the BET treatment of the adsorption data obtained at higher pressures ($0.05 < p/p_s < 0.2-0.3$). For this type of surface, immersion calorimetry can also be described within the framework of Dubinin's theory. Graphitized carbon blacks and manganese dioxide are two

*To whom correspondence should be addressed.

solids of industrial importance for which the DRK equation is observed.

2 Theoretical Background

Open and energetically homogeneous surfaces are relatively rare and most solids present some degree of porosity, within the traditional domains of microporosity, mesoporosity and macroporosity.^{1,12} From a molecular point of view, microporosity represents an extreme case and therefore one should establish a clear distinction between micropores and the rest of the surface. In view of the small dimensions of these pores (cavities of less than 2 nm in width), the adsorption energy is enhanced and consequently adsorption occurs first in these pores. In principle, no capillary condensation occurs in micropores, as opposed to the larger pores, where one observes a hysteresis loop on desorption.¹ Moreover, the volume of the micropores and the surface area of their walls are often quite high, which makes the corresponding solids very attractive for industrial applications.

2.1 Adsorption in micropores

Microporous structures are often associated with meso- and macropores, as observed with active carbons, and a purely external surface area where another type of adsorption occurs. We shall therefore begin with adsorption in micropores and outline briefly the main features of Dubinin's theory in its modern formulation. The basic expression is the equation of Dubinin and Astakhov (DA), postulated in 1971:⁴⁻⁶

$$N_a = N_{ao} \exp[-(A/E)^n] \quad (1)$$

where $A = RT \ln(p_s/p)$. The quantity N_a (usually in mmol g^{-1} of solid) is the amount adsorbed at relative pressure p/p_s and N_{ao} is the limiting amount filling the micropores. The latter is related to the micropore volume $W_o = N_{ao} V_m$ filled by the liquid-like adsorbate of molar volume V_m . In the case of narrow micropores, W_o strongly depends on the molecular size of the adsorbate.

The characteristic energy E depends on the chemical nature of the system and on the micropore size. In the case of microporous carbons and zeolites, $E = E_o \beta$, where the affinity coefficient β is a factor depending on the adsorbate. By convention $\beta(\text{C}_6\text{H}_6) = 1$.

The case where exponent $n = 2$, often found for typical active carbons, corresponds to the original equation of Dubinin and Radushkevich (DR). On the other hand, for other microporous solids such

as zeolites, n can vary between 2 and 4–5. From a theoretical point of view, E and n are related to the distribution of the adsorption energy in the micropore system. On the basis of molecular sieve experiments, it has been shown that for active carbons the characteristic energy E_o (kJ mol^{-1}) is related to the average width L of the slit-shaped micropores:⁶

$$L(\text{nm}) = 10.8 / (E_o - 11.4) \quad (2)$$

Typical values for E_o are found between 30–35 and 16–17 kJ mole^{-1} , which correspond to average pore-widths of approximately 0.4 to 2.5 nm.

As suggested by model calculations, an inverse relation between E and micropore dimensions must exist for systems other than carbons. This has been observed in the case of water adsorption by calcium and sodium montmorillonite,¹³ where the spacing between the layers increases stepwise with the amount of water adsorbed by the solid. As expected, E depends on the interlayer spacing and on the type of cation interacting with the water molecule, which leads to different correlations between E and L .

For slit-shaped micropores, as found in active carbons and in montmorillonites, the surface area of the pores is related to their volume and their width through

$$S_{mi}(\text{m}^2 \text{ g}^{-1}) = 2000 W_o(\text{cm}^3 \text{ g}^{-1}) / L(\text{nm}) \quad (3)$$

The presence of micropores in an unknown solid can be revealed by the analysis of the low pressure adsorption data using eqn (1). However, as this is not an absolute proof, it is often advisable to confirm the presence or the absence of microporosity by experiments based on molecular sieve effects. In this context, immersion calorimetry plays an important role. It is a relatively easy and rapid technique, described below. Another technique is the comparison of the adsorption isotherm with a reference isotherm,¹ obtained under similar conditions for a non-porous solid of the same chemical nature (for example, a graphitized carbon black in the case of carbons). This approach provides information on the approximate micropore volume and on the surface area found outside the micropores. Nowadays, direct evidence for the presence or the absence of microporosity can also be provided by STM or AFM.

2.2 Immersion calorimetry

Immersion calorimetry is a very useful complement to the adsorption of vapours and gases and it

provides direct information on the surface energy. The calorimeter used in our studies is of the Tian-Calvet type and allows the determination of energies between 2 and 50 Joules. Therefore, a minimum surface area of $5\text{--}10\text{ m}^2\text{ g}^{-1}$ is required, but more sensitive instruments exist.

By definition, the enthalpy of immersion is equal to the integral of the net heat of adsorption plus a term $S_{LV}h_{LV}$, taking into account the surface and the enthalpy of the liquid vapour interface ($h_{LV} < 0$). In the case of systems described by the theory of Dubinin, a standard thermodynamic treatment applied to eqn (1) leads to a general expression for Δh_i , the enthalpy of immersion of a microporous solid into a liquid. For the filling of a micropore system with virtually no liquid-vapour interface S_{LV} , the enthalpy of immersion is simply equal to the integral of the net heat of adsorption. Equation (1) leads to^{5,6}

$$\Delta h_i(\text{J g}^{-1}) = -N_{ao}E(1 + \alpha T)\Gamma(1 + 1/n) \quad (4)$$

α is the expansion coefficient of the adsorbate and Γ is the classical 'gamma' function. In the case of the DR equation, $n = 2$ and introducing the micropore volume $W_o = N_{ao}V_m$ accessible to the given molecule, eqn (4) finally becomes

$$\Delta h_i(\text{J g}^{-1}) = -\beta E_o W_o(1 + \alpha T)(\pi)^{1/2}/2V_m \quad (5)$$

A good correlation has been found between experimental and calculated values of Δh_i ,^{6,10} but an extra term $h_i S_e$ must be added to eqn (5) for the wetting of the external (non-microporous) surface of the solid S_e , so that

$$\Delta h_i(\text{exp}) = \Delta h_i(\text{micropores}) + h_i S_e \quad (6)$$

In most cases, the second term is a fraction of the first.

It has been shown recently,^{14,15} that eqn (1) also applies to type IV isotherms (S-shaped) and in particular to the case of water adsorption by active carbons. This offers new possibilities for the description of isotherms other than Types I (Langmuir) and II. However, as postulated by Dubinin's theory, parameters E and n must be temperature-invariant. This has been checked in the case of water adsorption, but it is not necessarily the case for Type IV isotherms in general.

As illustrated in Section 3, the combination of adsorption isotherm and immersion calorimetry provides useful information for the characterisation of microporous solids. Under favourable con-

ditions, immersion into liquids of molecular dimensions between 0.4 and 1.5 nm leads to micropore distributions in the corresponding range. As shown recently,^{16,17} gate effects can be revealed unambiguously by the combination of adsorption and immersion techniques. For example, the adsorption of a small molecule like CH_2Cl_2 (0.38 nm) may indicate an average pore-size of 1 nm or more, as given by eqn (2), but immersion into a liquid such as CCl_4 (0.63 nm) is unusually low. This suggests the presence of constrictions at the entrance of the micropores.

Immersion calorimetry can also be applied to investigate specific interactions on the surface of solids in general. In the case of non-porous solids, immersion into a liquid without specific interactions provides information on the specific surface energies h_i ,¹

$$h_i(\text{J m}^{-2}) = \Delta h_i(\text{J g}^{-1})/S(\text{m}^2 \text{ g}^{-1}) \quad (7)$$

The specific enthalpies of immersion h_i are usually derived by using the nitrogen BET area at -196°C . In the case of benzene, which shows no specific interactions, typical values of $-h_i(\text{C}_6\text{H}_6)$ are 0.114 (carbon blacks), 0.120 to 0.160 (silica) and 0.130 J m^{-2} (external surface of Ca and Na montmorillonites). Equation (7) can also be used to determine the surface area from the enthalpy of immersion, provided that no specific interactions take place.

In the case of specific interactions, which is frequently the case with water, immersion calorimetry provides complementary information on the state of porous and non-porous surfaces. Table 1 illustrates this point in the case of two non-porous illites investigated in our laboratory. The solids are of different origins but have identical crystallographic structures. The specific surface areas were determined by nitrogen adsorption at -196°C and immersions were carried out in *n*-hexane and water at 20°C .

This example shows that in the case of illites the surface area of powders of different origins can be assessed rapidly by immersion calorimetry into *n*-hexane, using the specific enthalpy value of $-73 \pm 1\text{ mJ m}^{-2}$. On the other hand, immersion into water provides a more refined picture of the

Table 1. Adsorption and immersion data for two non-porous illites

Origin	S_{BET} ($\text{N}_2; -196^\circ\text{C}$) ($\text{m}^2 \text{ g}^{-1}$)	$-\Delta h_i$ (C_6H_{14})/ S_{BET} (J m^{-2})	$-\Delta h_i$ (H_2O)/ S_{BET} (J m^{-2})
France	115	0.073	0.371
Hungary	34	0.074	0.782

state of the surface. By extension, the same approach applies to other non-porous solids.

2.3 Adsorption outside micropores

Adsorption which occurs outside micropores, that is in meso- and macropores and on purely open surfaces, is well described by a number of expressions, including the classical BET equation¹. The latter is a useful tool for the determination of the specific surface area, but it cannot be applied to micropore adsorption: in solids such as carbons and montmorillonites, the micropores of which may contain several layers. Consequently, the monolayer capacity N_{am} obtained from the BET analysis corresponds essentially to the monolayer equivalent of the volume filling the pores, and not the real surface area of the pores, given by eqn (3). In the case of microporous solids with a significant external surface area S_e , the latter can be assessed from a plot comparing the amounts adsorbed at the same pressures by the porous solid and a non-porous reference¹. It is also possible to subtract the Dubinin–Radushkevich isotherm from the overall isotherm and to analyse it separately, or to calculate S_e from eqn (6). As shown elsewhere, the different approaches are in reasonable agreement⁶.

As illustrated above for the two illites, the combination of the BET analysis with immersion calorimetry into liquids with non-specific interactions can lead to reliable information on non-porous solids. However, if the adsorption isotherm is known accurately, further refinements are possible. For example, several years ago, Kaganer^{1,11} pointed out that for a number of non-porous surfaces, the low pressure data could be fitted to an expression similar to the Dubinin–Radushkevich equation and later called the Dubinin–Radushkevich–Kaganer (DRK) equation:

$$N_a = N_{ao} \exp \left[- (RT \ln p_s/p)^2 / E^2 \right] \quad (8)$$

The fundamental difference between the two expressions is the fact that eqn (8) corresponds to adsorption on an open surface, as opposed to the filling of a micropore volume in the case of the DR equation. Strictly speaking, the temperature invariance of parameter E , implied by Dubinin's theory, should also apply to the DRK equation and it must be verified before further thermodynamic consequences are considered.

For the systems following the DRK equation, one finds that the limiting value N_{ao} derived from the low pressure region ($p/p_s < 10^{-2} - 10^{-3}$) is close to N_{am} , the statistical monolayer capacity derived from the BET analysis of the same isotherm but at higher relative pressures ($0.05 < p/p_s < 0.2 - 0.3$).

As illustrated below (Section 3), a systematic investigation carried out in our laboratory at temperatures between 8 and 40°C shows that the DRK equation applies to certain systems of industrial importance. As a consequence, the extension of Dubinin's theory to the enthalpies of immersion, expressed by eqn (4), must also hold. The corresponding expression, based on the DRK equation, is

$$\Delta h_i (\text{J g}^{-1}) = N_{ao} E (1 + \alpha^* T) (\pi)^{1/2} / 2 + S_{LV} h_{LV} \quad (9)$$

The liquid vapour interface S_{LV} is practically the surface of the non-porous solid and h_{LV} the surface enthalpy of the liquid–vapour interface ($h_{LV} < 0$); α^* is the two-dimensional expansion coefficient of the monolayer, theoretically equal to $2\alpha/3$. In the absence of high energy sites, not accounted for by the DRK analysis, eqn (9) should provide a test for self-consistency between the different techniques.

2.4 Fractal analysis of open surfaces

In the case of open but irregular surfaces, further information can be obtained through the fractal character D ($2 < D < 3$) of the surface, if present at all. This approach is discussed in the collective work edited by Avnir¹⁸ and, for example, in Feder's monograph.¹⁹ Some aspects of fractal geometry are of direct interest in the characterisation of solids. For example, for powders containing spherical particles of radius R , the specific surface area is^{20,21}

$$S_R (m^2 g^{-1}) \sim R^{(D-3)} \quad (10)$$

as opposed to R^{-1} for smooth spheres, where $D = 2$. The fractal character of the surface may therefore lead to differences between real and calculated specific areas, assuming a smooth surface. For particles of radius R , the ratio is equal to R^{D-2} and it expresses the roughness of the real surface. This property must be taken into account when assessing the total surface area of a powder with a distribution of particle sizes. In fact, D can be evaluated by fitting the total surface area derived from the particle size distribution, obtained from image analysis, to the experimental surface area of the powder. This relatively simple approach is under investigation in our laboratory.

At the level of molecular dimensions, the fractal character of a surface D can be estimated by different techniques. For example, from the adsorption of molecular probes with different

molecular surface areas, following the relation proposed by Avnir^{20,21}

$$\ln(N_{am}) \sim -(D/2) \ln(\sigma) \quad (11)$$

where N_{am} is the statistical monolayer derived from the BET model.

Another approach, which can be applied to single adsorption isotherms, is the fit to a modification of the classical BET equation,¹³ proposed by Fripiat, and taking into account the influence of the fractal character on the successive layers²²

$$N_a(x)/N_{am} = [c \sum i^{2-D} (\Sigma x^i)] / [1 + c \Sigma x^i] \quad (12)$$

In this expression, $x = p/p_s$ and the summations vary from $i = 1$ to an arbitrary limit m (at least 5–10), depending on the convergence of the series.

For graphitized carbon blacks with $D < 2.4$ – 2.5 , good correlation has been observed between the results obtained from eqns (11) and (12), but the validity is limited to dimensions below 5–10 nm. However, good agreement has been found with the fractal character derived from small angle X-ray scattering (SAXS).^{19,23} More recently, analysis of the STM/AFM signal has also been considered in our laboratory.²⁴ These techniques have the advantage that they cover a wider range of dimensions on the surface. It is therefore possible to confirm the presence and the extent of the fractal character suggested by eqns (11) and (12).

In the technique based on the analysis of the STM and AFM pictures, the fractal dimension of the surface—if present at all—is revealed by the shape of the power spectrum of the profiles (1-dimensional signal) or the surface itself (2-dimensional signal). This information is obtained through a Fourier transform of the STM/AFM signal, carried out on different patches, which provides a statistically reliable sampling of the surface. For the one-dimensional analysis of the profile $Z(x)$, the basic equation is

$$Z(x) = \int_{-\infty}^{+\infty} F(f) \exp[2\pi i x f] df \quad (13)$$

The corresponding power spectrum is $F(f)$. $F^*(f) = |F(f)|^2$, obtained from the inverse Fourier transform. If $Z(x)$ is fractal, the power spectrum is proportional to $f^{-\beta}$, where β is related to D .²⁵ The fractal dimension of the profile is $D_1 = (5 - \beta)/2$, a value between 1 and 2, and it can be shown that this should correspond to a surface fractal dimension

$D = D_1 + 1$. On the other hand, the Fourier transform of the two-dimensional STM picture leads directly to $D = (7 - \beta)/2$. At high magnification, the STM/AFM pictures also provide useful information on the state of the surface, by revealing directly the presence or the absence of micropores. As shown in Section 3, these observations can be correlated with indirect determinations based on adsorption and immersion techniques.

3 Applications Based on the Different Techniques

The present section illustrates the possibilities offered by the combination of adsorption and immersion techniques combined with AFM/STM. Typical examples have been selected in field of active carbons, carbon blacks and manganese dioxide, solids of industrial importance.

3.1 Active carbons

Active carbon CMS, of industrial origin and used in filtration processes, has been subjected to a thorough investigation.^{5,6,14} The main characteristics, derived from vapour adsorption isotherms and from immersion calorimetry at 20°C, are given in Table 2.

As shown in detail elsewhere,^{6,17} the enthalpies of immersion into eight organic liquids with molecular dimensions between 0.41 and 1.5 nm lead to the distribution of the micropore volume dW/dL , shown in Fig. 1. The histogram suggests an average near 0.9 nm, in good agreement with 0.7 nm, the value calculated from eqn (2).

Examination of the surface by STM (Figs 2 and 3) reveals the entrances to the micropores and the

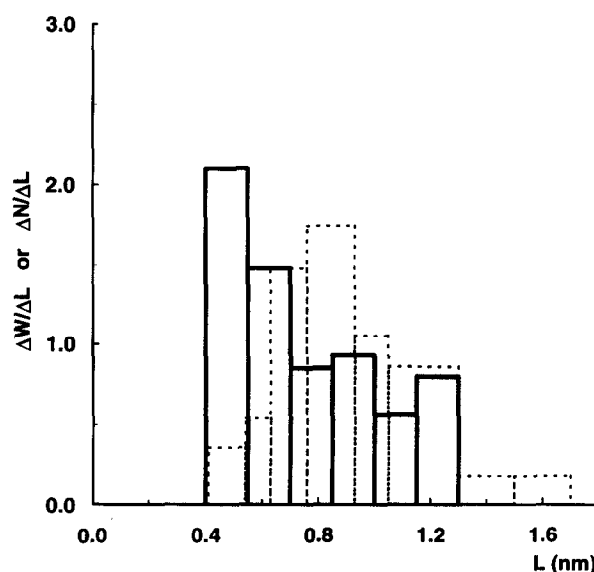


Fig. 1. Micropore distributions in active carbon CMS obtained from molecular sieve experiments, dW/dL (dotted line), and from STM analysis of the surface, dN/dL (solid line). L is the width of the slit-shaped micropores.

Table 2. Main characteristics of active carbon CMS. Tetrabutylurea (TBU) and tri-2,4 xylylphosphate (TXP) have critical diameters of 0.93 and 1.5 nm, respectively

$W_o(C_6H_6)$ ($cm^3 g^{-1}$)	E_o ($kJ mole^{-1}$)	L (nm)	S_{mi} ($m^2 g^{-1}$)	S_e ($m^2 g^{-1}$)	$-\Delta h_i(C_6H_6)$ ($J g^{-1}$)	$-\Delta h_i(TBU)$ ($J g^{-1}$)	$-\Delta h_i(TXP)$ ($J g^{-1}$)	$-\Delta h_i(H_2O)$ ($J g^{-1}$)
0.252	26.2	0.73	685	25	92	40	4.5	27.5

statistical distribution of their widths, dN/dL can be obtained from the analysis of the surface profiles. As shown in Fig. 1, the distributions dW/dL and dN/dL are similar, but not identical. This is not too surprising and indicates that the micropores are not affine. It is interesting to point out that a good agreement has been observed for other carbons, dN/dL being determined from transmission electron microscopy at high resolution.^{6,26}

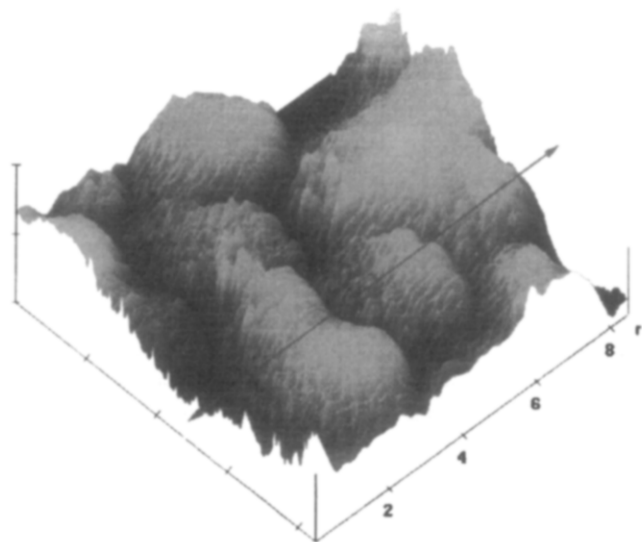
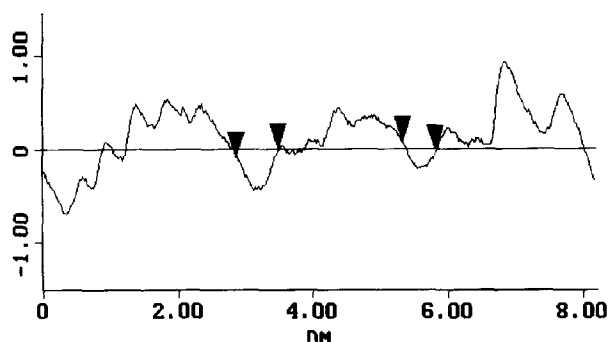
In the case of carbon CMS, the adsorption of water corresponds to an S-shaped isotherm,¹⁴ corresponding to type V in the standard classification.¹ This isotherm can be fitted to the Dubinin-Astakhov eqn (1) with $E = 1.86 kJ mol^{-1}$ and $n = 4.20$. The enthalpy of immersion calculated through eqn (4) leads to $-27 J g^{-1}$, in agreement with the experimental value of $-27.5 J g^{-1}$ given in Table 2. Consequently, for this solid a full characterisation can be obtained from the different techniques.

3.2 Adsorption by non-porous carbons blacks and manganese dioxide

According to Dubinin,⁴ the adsorption of benzene on carbon blacks and on the external surface of active carbons is described by eqn (1) with exponent $n = 1$ and A in $kJ mol^{-1}$

$$N_a = 9.16 \times 10^{-6} \exp[-(A/6.35)] mol m^{-2} \quad (14)$$

However, this observation is based on a single temperature (20°C) and the monolayer capacity of

**Fig. 2.** STM micrograph of the surface of active carbon CMS.**Fig. 3.** Typical STM profile for the surface of active carbon CMS, perpendicular to the slit-shaped micropores of 0.63 and 0.48 nm seen in Fig. 2. For technical reasons, the information on the depth of the micropore (vertical axis) is not true.

$9.16 \times 10^{-6} mol m^{-2}$ corresponds to a molecular surface area $A_m(C_6H_6) = 18 \times 10^{-20} m^2$. This value is approximately half the standard value,¹ derived from the BET range, and based on $16.2 \times 10^{-20} m^2$ for the nitrogen molecule, which suggests some inconsistency in the model. Recent studies carried out in our laboratory, show that the adsorption of benzene on a typical carbon black (Hoechst) at 9, 20 and 37°C is well described by the DRK eqn (8); as illustrated by Fig. 4, one obtains a single line for the plot of $\ln(N_a)$ versus $A^2 = (RT \ln p/p_s)^2$, with a slope corresponding to $E = 11 kJ mole^{-1}$. The latter is also close to the limiting value of $11.4 kJ mole^{-1}$, which appears in eqn (2) and corresponds formally to a flat surface.

The average value of N_{ao} ($0.27 mmol g^{-1}$) is in good agreement with the value of N_{am} ($0.21 mmol g^{-1}$) derived from the BET treatment at higher relative pressures. With the molecular surface area of $42 \times 10^{-20} m^2$, one obtains a specific surface area of $52 m^2 g^{-1}$.

A similar agreement with the DRK equation is observed with nitrogen adsorbed at $-196^\circ C$, leading to $E = 6.4 kJ mole^{-1}$ and $N_{ao} = 0.574 mmol g^{-1}$, which corresponds to $56 m^2 g^{-1}$. It is close to $52 m^2 g^{-1}$, obtained from the BET range. These examples show consistency between the BET and DRK approaches for the adsorption of vapours on various non-porous surfaces.

Since E appears to be temperature invariant, it follows that eqn (9) must be valid. Using $\alpha^*(C_6H_6) = 0.83 \times 10^{-3} K^{-1}$, $h_{LV}(C_6H_6) = -0.068 J m^{-2}$ and $S = 52 m^2 g^{-1}$ one obtains $\Delta h_i(C_6H_6) = 5.8 J g^{-1}$ against $5.65 \pm 0.35 J g^{-1}$ experimentally.

These results show that, in the case of carbonaceous surfaces, eqn (14) can probably be replaced by

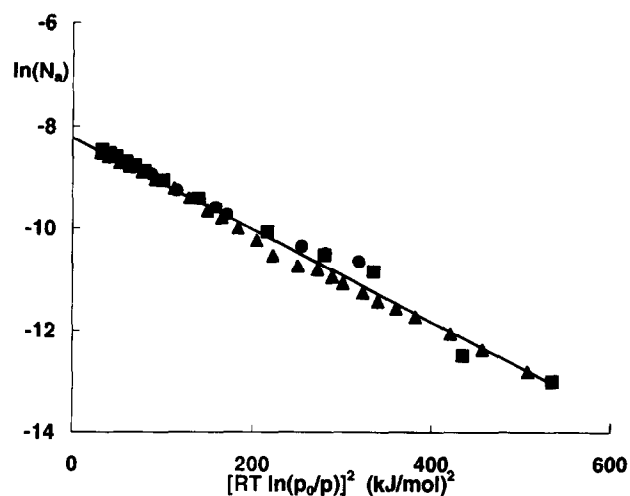


Fig. 4. Logarithmic plots of the DRK eqn (8) for the adsorption of benzene at 9°C (●), 20°C (▲) and 37°C (■) on carbon black 'Hoechst'. The nitrogen BET surface area is $52 \text{ m}^2 \text{ g}^{-1}$.

the DRK eqn (8). This may lead to a more rational description for the adsorption of vapours such as benzene, by porous and non-porous carbons.

Similar observations are made for the adsorption of nitrogen at -196°C and of CH_2Cl_2 at 5, 20 and 41°C on non-porous $\alpha\text{-MnO}_2$ (Fig. 5). For dichloromethane, the logarithmic plot of the DRK equation leads to a single straight line, which indicates temperature invariance of E in the corresponding interval. One obtains the average values $E = 17 \text{ kJ mol}^{-1}$ and $N_{ao} = 0.31 \text{ mmol g}^{-1}$. The BET treatment of the isotherm at 20°C leads to $N_{am} = 0.28 \text{ mmol g}^{-1}$. Since $S_{BET}(\text{N}_2) = 62 \text{ m}^2 \text{ g}^{-1}$, one obtains a molecular surface area of $35 \times 10^{-20} \text{ m}^2$ for CH_2Cl_2 on $\alpha\text{-MnO}_2$. It is somewhat larger than the value of $29 \times 10^{-20} \text{ m}^2$ calculated from the liquid density. The enthalpy of immersion calculated with eqn (9) is $\Delta h_i(\text{CH}_2\text{Cl}_2) = -10 \text{ J g}^{-1}$ against -14 J g^{-1} experimentally. The difference may be due to the

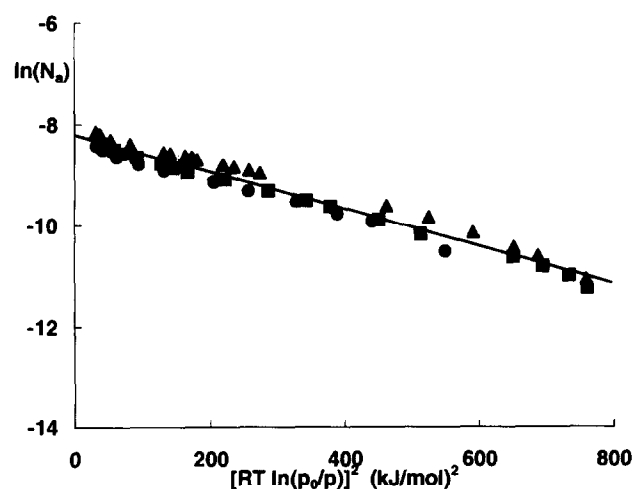


Fig. 5. Logarithmic plots of the DRK eqn (8) for the adsorption of dichloromethane at 5°C (●), 20°C (▲) and 41°C (■) on $\alpha\text{-MnO}_2$. The nitrogen BET surface area is $62 \text{ m}^2 \text{ g}^{-1}$.

presence of high energy sites outside the DRK range and not accounted for by eqn (9). The applicability of the DRK model to non-porous surfaces, with its thermodynamic consequences, is also under investigation and further results will be reported in due course.

3.3 The fractal character of carbon black surfaces as a model case

As revealed by different studies, the surface of carbon blacks can be fractal and D tends towards 2 for well graphitized samples.^{20,21} Obviously, fractal geometry is not a general property of solid surfaces, but the observations made with a series of carbon blacks illustrate the possibilities offered by adsorption measurements and other techniques such as AFM/STM and small-angle X-ray scattering when a surface has a fractal geometry.

A typical carbon black, XYL, obtained by thermal decomposition of xylene and tested for use in dry cells of the 'Leclanché' type (Zn/MnO_2) was subjected to this type of analysis. As shown in Table 3, with Fripiat's eqn (12), the adsorption of nitrogen at -196°C and of CH_2Cl_2 at 20°C lead to an average fractal coefficient $D = 2.25 \pm 0.05$.

Sample XYL was also subjected to small-angle scattering of X-rays (SAXS) and the logarithmic plot of the intensity J versus the scattering angle φ , leads to a straight line (Fig. 6). According to the theory,^{19,23} the slope is equal to $D - 6$, which leads to $D = 2.31 \pm 0.02$. A similar agreement has also been found for graphitized black N-234-X, with values of D between 2.10 and 2.15 for Fripiat's method and SAXS.

In the case of sample XYL, a systematic analysis of the STM signal was carried out by applying eqn (13) and its two-dimensional analogue. A typical STM profile consisting of 400 points measured

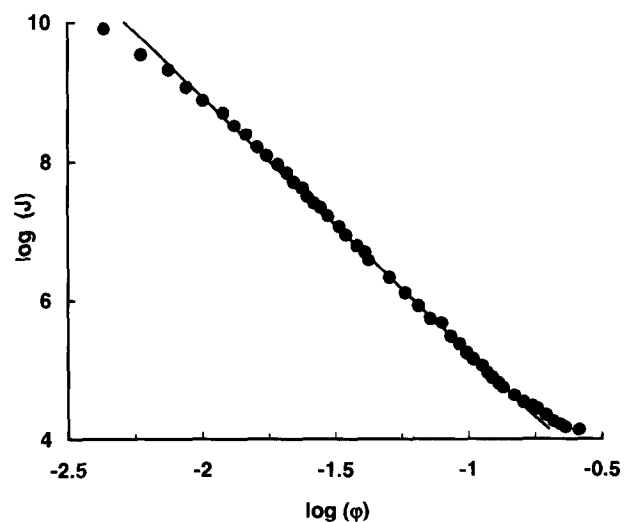


Fig. 6. Small angle X-ray scattering of X-rays by carbon black XYL (logarithmic coordinates), leading to the fractal coefficient $D = 2.31 \pm 0.02$ of its surface.

Table 3. Fractal coefficient D for the surface of carbon black XYL, obtained from different techniques. (In the case of the profile analysis, one must add 1 to the value of D to obtain the fractal character of the surface)

Technique	Gas adsorption	SAXS	Profile FT	Selected area FT
D	2.25 ± 0.05	2.31 ± 0.02	1.32 ± 0.06	2.23 ± 0.10

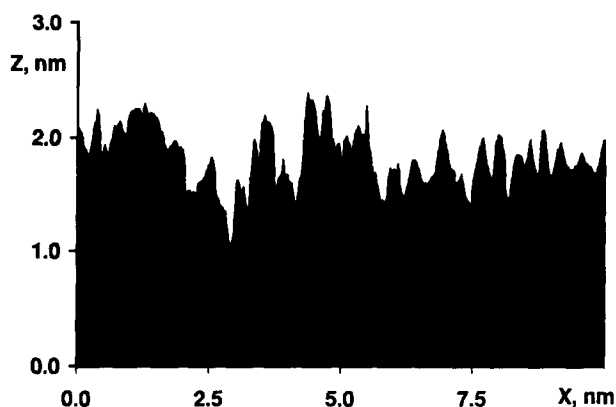


Fig. 7. Typical STM profile $Z(x)$ measured on the surface of carbon black XYL over a distance of 10 nm (400 points). The Fourier transform (13) leads to the fractal character of the profile.

over a horizontal distance of 10 nm is shown in Fig. 7. The Fourier transforms (FT), carried out on 3192 profiles and on eight different regions of 5×5 to $15 \times 15 \text{ nm}^2$ lead to a statistical distribution of D over the surface, with a standard deviation $\pm \sigma_D$. As shown in Table 3, the different techniques are in good agreement for this type of surface. However, each technique has its shortcomings and therefore one may expect discrepancies for certain systems. The present example is almost an ideal case.

4 Conclusions

The present paper shows that an increasing degree of information can be obtained in the characterisation of powder when combining standard adsorption measurements with immersion calorimetry and AFM/STM studies. For routine investigation of relatively well-known materials and limited to adsorption, care must be taken to establish the presence or the absence of microporosity. This can be achieved by using a reference isotherm. On the other hand, for new compounds, it is advisable to include calorimetry, to confirm adsorption data and to obtain surfaces energies. New techniques such as AFM and STM, should also be considered, in view of the variety of information gained by direct observation of the surface at molecular scale.

It is also interesting to examine the extension of Dubinin's theory to certain types of open surfaces, in

the form of the DRK eqn (8) and its thermodynamic consequence eqn (9).

Acknowledgements

The authors wish to thank the Swiss National Science Foundation's M. Heim-Vocgtlin Stiftung (D. Hugi-Cleary) and the Spanish Consejo Superior de las Investigaciones Científicas (T. A. Centeno) for financial support while working at Neuchâtel University. Thanks are also due to Dr G. M. Plavnik, Institute for Physical Chemistry, Russian Academy of Sciences, Moscow, for SAXS measurements on carbons blacks, and to Dr T.K. Wang, University of Mulhouse (France) for his collaboration in the field of AFM/STM.

References

1. Gregg, S. and Sing, K. S. W., *Adsorption, Surface Area and Porosity*, 2nd edn. Academic Press, London, 1982.
2. Parfitt, G. D. and Sing, K. S. W., *Characterisation of Powder Surfaces*. Academic Press, London, 1976.
3. Rudzinski, W. and Everett, D. H., *Adsorption of Gases on Heterogeneous Surfaces*. Academic Press, London, 1992.
4. Dubinin, M. M., *Fundamentals of the theory of adsorption in microporous solids*. *Carbon*, 1989, **27**, 457–467.
5. Stoeckli, F., Dubinin's theory for the volume filling of micropores. *Adsorption Science and Technology*, 1993, **10**, 3–16.
6. Stoeckli, F. in *Porosity in Carbons*, ed. J. W. Patrick. Edward Arnold, London, 1995, pp. 67–92, Ch. 3.
7. Lavanchy, A., Stöckli, M., Wirz, C. and Stoeckli, F., Binary adsorption of vapours in active carbons described by the Dubinin equation. *Adsorption Science and Technology*, 1996, **13**, 537–545.
8. Stoeckli, F., Wintgens, D., Lavanchy, A. and Stöckli, M., Binary adsorption in active carbons described by the combined theories of Myers–Prausnitz and Dubinin (II). *Adsorption Science and Technology*, 1997, **15**, 677–683.
9. Lavanchy, A. and Stoeckli, F., Dynamic adsorption of vapour mixtures in active carbons. *Carbon*, 1997, **35**, 1573–1579.
10. Stoeckli, F. and Kraehenbuehl, F., The enthalpies of immersion of active carbons in relation to the Dubinin theory for the volume filling of micropores. *Carbon*, 1981, **19**, 353–356.
11. Kaganer, M. G., A method for the determination of specific surfaces from the adsorption of gases (English translation). *Proceedings of the USSR Academy of Sciences*, 1957, **116**, 603–605.
12. Everett, D. H., Definitions, terminology and symbols in colloid surface chemistry. *Pure and Applied Chemistry*, 1972, **31**, 579–638.
13. Kraehenbuehl, F., Stoeckli, F., Brunner, F., Kahr, G. and Müller-Von Moos, Study of the water–bentonite system by water adsorption, immersion calorimetry and X-ray techniques. *Clay Minerals*, 1987, **22**, 1–9.
14. Stoeckli, F., Jakubov, T. S. and Lavanchy, A., Water adsorption in active carbons described by the Dubinin–Astakhov equation. *J. Chem. Soc. Faraday Trans.*, 1994, **90**, 783–786.
15. Stoeckli, F., Currit, L., Laederach, A. and Centeno, T. A., Water adsorption in carbons described by the Dubinin–Astakhov equation. *J. Chem. Soc. Faraday Trans.*, 1994, **90**, 3689–3691.

16. Centeno, T. A. and Stoeckli, F., The oxidation of an Asturian bituminous coal in air and its influence on subsequent activation by steam. *Carbon*, 1995, **33**, 581–586.
17. Stoeckli, F. and Centeno, T. A., On the characterisation of microporous carbons by immersion calorimetry alone. *Carbon*, 1997, **35**, 1097–1100.
18. Avnir, D. (ed.), *The Fractal Approach to Heterogeneous Chemistry*. John Wiley and Sons, Chichester, UK, 1989.
19. Feder, J., *Fractals*. Plenum Press, New York, 1989.
20. Avnir, D., Farin, D. and Pfeifer, P., Chemistry in non-integer dimensions between two and three. Fractal surfaces of adsorbents. *J. Chem. Phys.*, 1983, **79**, 3566–3571.
21. Farin, D. and Avnir, D., The fractal nature of molecule-surface interactions. In *The Fractal Approach to Heterogeneous Chemistry*, ed. D. Avnir. John Wiley & Sons, Chichester, UK, 1989, pp. 271–284.
22. Fripiat, J. J., Porosity and adsorption isotherms. In *The Fractal Approach to Heterogeneous Chemistry*, ed. D. Avnir. John Wiley & Sons, Chichester, UK, 1989, pp. 331–340.
23. Schmidt, P. W., Use of scattering to determine the fractal dimension. In *The Fractal Approach to Heterogeneous Chemistry*, ed. D. Avnir. John Wiley & Sons, Chichester, UK, 1989, pp. 67–79.
24. Stoeckli, F. and Currit, L., The fractal character of surfaces determined by Fourier analysis of STM data. *Carbon*, 1993, **33**, 338–340.
25. Voss, R. F. and Saupe, D., *The Science of Fractal Images*, ed. H. D. Peitgen and D. Saupe, Springer-Verlag, New York, 1988, pp. 22–113.
26. Innes, R., Fryer, J. and Stoeckli, F., On the correlation between micropore distributions obtained from molecular probes and from high-resolution electron microscopy. *Carbon*, 1989, **27**, 71–76.